Carbohydrate Polymers 83 (2011) 1311–1321

Contents lists available at ScienceDirect

Carbohydrate Polymers

journal homepage: www.elsevier.com/locate/carbpol

Synthesis and characterization of thiolated alginate-albumin nanoparticles stabilized by disulfide bonds. Evaluation as drug delivery systems

A. Martínez[a], I. Iglesias[a], R. Lozano[b], J.M. Teijón[c], M.D. Blanco[c,*], Group of Polymeric Materials for the Controlled Release of Bioactive Compounds in Biomedicina

[a] Departamento de Farmacología, Facultad de Farmacia, Universidad Complutense de Madrid, Spain
[b] Departamento de Química inorgánica y Bioinorgánica, Facultad de Farmacia, Universidad Complutense de Madrid, Spain
[c] Departamento de Bioquímica y Biología Molecular, Facultad de Medicina, Universidad Complutense de Madrid, Spain

ARTICLE INFO

Article history:
Received 18 March 2010
Received in revised form
21 September 2010
Accepted 22 September 2010
Available online 29 September 2010

Keywords:
Nanoparticles
Alginate
Albumin
Tamoxifen
Drug delivery systems

ABSTRACT

Nanoparticles based on thiolated alginate (ALG-CYS) and disulfide bond reduced albumin (BSA-SH) have been synthesized by coacervation method and stabilized by disulfide bond formation. In order to optimize the synthesis, the influence of amount and proportion of reactants on nanoparticle characteristics has been studied. Results showed cubic shaped nanoparticles but with a certain spherical tendency. The size range was 42–388 nm; as the percentage of ALG-CYS increased in the particle, their morphology is less spherical and the size is larger. The presence of both reactants in the nanoparticles was determined by FT-IR and confirmed by TGA. The ratio BSA-SH/ALG-CYS (0.49/1–1.23/1) in the particles was quantified by colorimetric methods. Nanoparticles were assayed as drug delivery systems by loading them with tamoxifen (TMX) (2–4 μg TMX/mg NP). Maximum TMX release (23–61% of loaded TMX) took place between 7 and 75 h, and the amount of released TMX can be modulated with the percentage of ALG-CYS in the particle.

1. Introduction

Research into the rational delivery of anticancer drugs is at the forefront of projects in nanomedicine. One of the major problems facing cancer chemotherapy is the achievement of the required concentration of the drug at the tumour site for a desired period of time (Chawla & Amiji, 2002). The vascularization of solid tumours is heterogeneous, showing poorly perfused regions as well as dense vascularized regions where a rapid growth occurs. Tumours usually present resistances to treatment due to both cellular and non-cellular mechanisms (Brigger, Dubernet, & Couvreur, 2002).

However, the leaky defective blood vessels of tumour tissue make its vasculature permeable to macromolecules in the size range from 100 to 1200 nm in diameter (Kratz, 2008). Thus, nanocarriers can be administered close to the tumour cells to achieve a localised action. Furthermore, nanoparticles protect the drug from degradation following administration, and drug solubility issues can be overcome, a particular advantage because large proportions of new drug candidates are water insoluble (Moghimi, Hunter, & Murray, 2005).

Various macromolecular substances, such as synthetic and natural polymers, can be used for nanoparticle preparation. Among natural polymers, serum albumin and sodium alginate are emerging as versatile carriers for drug targeting. The properties of these natural polymers, such as their ready availability, versatility and biodegradability, make them ideal candidates for their use in drug delivery systems. Thus, they have been used in a multitude of studies of nanoparticle preparation, some of them including anticancer drugs such as methotrexate (Kratz, 2008) or paclitaxel (Karmali et al., 2009; Yoshioka et al., 2007).

In the case of oestrogen-dependent breast cancer, a large number of molecules classified as "selective oestrogen receptor modulators" (SERMs) have been widely used. Tamoxifen is the most important member of this family of SERMs, and it has been successfully used since 1970s in treatment of hormone dependent breast cancer (Ameller, Legrand, Marsaud, & Renoir, 2004). However, tamoxifen shows a low water solubility, which limits the administration of this drug only to the oral route. Furthermore, following a long-term therapy, tamoxifen has some side effects, such as endometrial cancer and development of drug resistance. To overcome the undesirable side effects of tamoxifen, and to increase the concentration at the tumour site, tamoxifen could be entrapped in polymeric nanoparticles, which may provide a better means of delivery in terms of enhanced uptake by the tumour and increased local concentration of the drug at the receptor site (Chawla & Amiji, 2002).

* Corresponding author. Tel.: +34 913941447; fax: +34 913941691.
E-mail address: mdblanco@med.ucm.es (M.D. Blanco).

0144-8617/$ – see front matter © 2010 Elsevier Ltd. All rights reserved.
doi:10.1016/j.carbpol.2010.09.038

In the present study, nanoparticles based on disulfide bond reduced albumin (BSA-SH) and thiolated alginate (ALG-CYS) were prepared and stabilized by disulfide bonds formation, in order to characterize and to evaluate them as possible delivery systems of tamoxifen.

2. Materials and methods

2.1. Materials

Alginic acid sodium salt, Comassie Blue G-250, L-cysteine (non animal source), 5,5′-dithiobis(2-nitrobenzoicacid)(DTNB), 1-ethyl-3-(3-imethylaminopropyl)carbo-diimide hydrochloride (EDAC), potassium bromide (KBr, FT-IR grade), 2-mercaptoethanol (2-ME) and tamoxifen were purchased from Sigma–Aldrich (Barcelona, Spain). Sodium hydroxide (NaOH), hydrochloric acid (HCl, 35%), potassium dihydrogen phosphate (KH_2PO_4), dipotassium hydrogen phosphate (K_2HPO_4), ethanol absolute, trichloroacetic acid, urea, phosphoric acid (88%), triethylamine and methanol (HPLC gradient grade) were purchased from Panreac (Barcelona, Spain). Sodium chloride (NaCl), bovine serum albumin (BSA, Fraction V), and sodium dodecyl sulfate were purchased from Merck (Barcelona, Spain).

2.2. Methods

2.2.1. Preparation of disulfide bond reduced bovine serum albumin (BSA-SH)

An aqueous solution of BSA 5% (w/v) was prepared. The pH-value was adjusted to 8 with 1 M NaOH (pH-meter METROHM 654). 70 μl of 2-mercaptoethanol (2-ME) was added and the resulting solution was incubated for 5 h under continuous stirring (100 rpm) at 37 °C. Thereafter, the pH-value was adjusted to 2.5 with 1 M HCl and the acidic solution was transferred to a dialysis bag (Visking® dialysis tubing 20/32 diameter: 16 mm, SERVA). The solution was exhaustively dialyzed against HCl solution (pH 3.5). The obtained solution was freeze dried for 24 h at −110 °C (Heto PowerDry LL1500 Freeze Dryer, Thermo Electro Corporation). The lyophilized product was conserved at 4 °C until further use.

2.2.2. Preparation of alginate-cysteine conjugate (ALG-CYS)

Alginate-cysteine conjugate was synthesized according to the methodology developed by Bernkop-Schnürch, Kast, and Richter (2001). The obtained alginate-cysteine conjugate was conserved at 4 °C until further use.

2.2.3. Determination of the thiol group content

The thiol concentration on the modified products was determined by a colorimetric reaction using Ellmanĭs reagent [DTNB] (Ellman, 1959; Marschütz & Bernkop-Schnürch, 2002). In this reaction, the free thiol groups of the polymers react with DTNB forming a coloured conjugate whose absorbance can be measured at 412 nm (UNICAM 8700 series UV/vis spectrometer). In brief, 0.5 mg of each conjugate was hydrated in 500 μl of 0.5 M phosphate buffer pH 8.0. After incubation for 2 h at room temperature with 500 μl of Ellmanĭs reagent [0.03% (w/v) DTNB in 0.5 M phosphate buffer pH 8.0], absorbance of the samples was measured at 412 nm. The amount of thiol groups of BSA-SH was calculated using a standard curve obtained from the sulfhydryl group determination of solutions containing increasing amounts of cysteine (0.003–0.05 mg/ml). The amount of thiol groups of ALG-CYS was calculated using a standard curve obtained from the sulfhydryl group determination of increasing amounts of cysteine solutions (0.003–0.05 mg/ml) containing a constant concentration of unmodified alginate (0.5 mg/ml).

2.2.4. Preparation of nanoparticles

Nanoparticles of BSA-SH and BSA-SH/ALG-CYS mixtures were prepared. Stabilization of nanoparticles was obtained by forming disulfide bonds. An initial protocol for synthesis was designed (Table 1; Experiment 1): 10 mg of BSA-SH and 10 mg of ALG-CYS were dissolved in 2 ml 1 mM HCl under intense stirring conditions. The obtained suspension was sonified (Branson sonifier 450) and the pH of the suspension was adjusted to 6.5–6.8 with 1 M NaOH. The formation of disulfide bonds was allowed to proceed for 12 h under intense stirring conditions. After this time, the resulting suspension was centrifuged (41,000 rpm, 15 min, Beckman Coulter Optima L-100 XP Ultracentrifuge), and the pellet was freeze dried for 24 h at −110 °C. Nanoparticles based only on BSA-SH and based only on ALG-CYS were prepared as described above (Table 1; Experiments 2 and 3).

Two different methods were proposed for the optimization of the process to avoid the aggregation tendency of the particles. The first alternative consisted of blocking the remaining free sulfhydryl groups of the nanoparticles with L-cysteine. 5 ml of a solution of L-cysteine (0.06 mM) was added and the reaction was allowed to proceed for 5 h under stirring conditions. After this time, the protocol was continued as above described (Table 1; Experiment 4). The second alternative consisted of stabilizing the particles with temperature, following previous desolvation with ethanol (Weber, Coester, Kreuter, & Langer, 2000). 0.5 ml of the suspension of particles was centrifuged (41,000 rpm, 15 min) and the pellet was suspended in an ethanol/water solution (1.2/0.3 ml/ml). This suspension was incubated at 70 °C for 2 h under stirring conditions. After this time, the suspension was centrifuged (41,000 rpm, 15 min) and the pellet was freeze dried (Table 1; Experiment 5).

Proportion and amount of initial reactants were studied as variables in the process of synthesis. Two more syntheses were prepared varying only the amount of initial reactants (Table 1, Experiments 6 and 8), and another one varying the proportion and the weight of reactants (Table 1; Experiment 7). According to the obtained results, in these three last experiments blocking of free sulfhydryl groups with L-cysteine was carried out.

2.2.5. Size and morphology of nanoparticles

The size and appearance of microspheres were studied by scanning electron microscopy (FE-SEM) (Jeol JSM-6400 Electron Microscope, resolution 36 mm from Centro de Microscopía y Citometría, UCM). From FE-SEM micrographs, more than 500 particles were measured using micrographs enlargements. The number-average diameter (D_n), the weight-average diameter (D_w) and the polydispersity index (U) were calculated (Guerrero et al., 2008). The particle distribution is considered to be monodisperse when U is between 1.0 and 1.1.

The size distribution analysis was performed on a back-scattered quasi-elastic light scattering device (Zetatrac NPA-152, Microtrac). Data were processed with Microtrac Flex software. According to the obtained results, average diameter and size distribution were only studied in particles of B-50-50, C-70-30 and BSA-SH synthesis (Table 1; Experiments 6, 7 and 8, respectively).

2.2.6. Composition of nanoparticles

The composition of BSA-SH/ALG-CYS particles was studied measuring the concentration of BSA-SH and ALG-CYS in the supernatant obtained after centrifugation of the samples in the synthesis process. The difference between the initial concentration of each polymer and their concentration in the supernatant was determined, and these amounts were considered to participate in nanoparticle formation.

Concentration of ALG-CYS in the supernatant was determined by measuring the absorbance of the coloured products obtained after a hydrolysis reaction of alginate. The hydrolysis of alginate

Table 1
Variables considered in the synthesis of nanoparticles.

Experiment number	Formulation	Total weight of initial reactants (mg)	Volume of dissolution (ml)	% (w/w) ALG-CYS	Blocking with L-cys	Temperature and desolvation with ethanol
1	A-50-50	20	2	50	–	–
2	BSA-SH	20	2	–	–	–
3	ALG-CYS	20	2	100	–	–
4	A-50-50	20	2	50	Yes	–
5	A-50-50	20	2	50	–	Yes
6	B-50-50	200	20	50	Yes	–
7	C-70-30	200	20	70	Yes	–
8	BSA-SH	200	20	–	Yes	–

was carried out in extreme conditions (10 N HCl, 5 h, 100 °C) and, after this reaction, samples were neutralised with 10 N NaOH and cooled. Absorbance of the samples was measured at 277.6 nm. A standard curve of ALG-CYS and another one of commercial alginate (0.5–4 mg/ml) were prepared to study possible differences between both materials in the hydrolysis reaction.

Concentration of BSA-SH in the supernatant was determined using Bradfordĭs method (Bradford, 1976). The absorbance of blue-coloured products of this reaction can be measured at 595 nm. To avoid interactions between alginate and Bradford reagent, BSA-SH in the supernatant was precipitated with 2 M trichloroacetic acid (TCA). After the precipitation process, samples were centrifuged and the supernatant was removed. The pellet was suspended in 1 ml 6 M urea (urea solution in 2 N HCl). A standard curve of BSA-SH and another one of commercial BSA (0.125–0.5 mg/ml) were prepared to study possible differences between both materials.

2.2.7. FT-IR spectroscopy

Modified materials and BSA-SH/ALG-CYS nanoparticles were analyzed by FT-IR spectroscopy and the resulting spectra were compared with the FT-IR spectra of the unmodified materials. For this study, a Nicolet Magna IR 750 Series II equipment with a DTGS-KBr detector was used. The measurement was realized preparing tablets with 300 mg of KBr and 2 mg of sample. Spectra were obtained at 4 cm^{-1} of resolution.

2.2.8. Preparation of tamoxifen-loaded nanoparticles

After centrifugation in the synthesis process, the obtained pellet was suspended in 2 ml of a 150 μg/ml TMX solution (in ethanol) and it was incubated for 12 h at room temperature. Then, the suspension was centrifuged (41,000 rpm, 15 min) and the pellet was freeze-dried. The supernatant was conserved for later characterization studies. All of the experiments with TMX were performed under subdued light as the drug is highly photosensitive. According to the obtained results, particles of B-50-50 (Table 1; Experiment 6), C-70-30 (Table 1; Experiment 7) and BSA-SH synthesis (Table 1; Experiment 8) were selected for loading the drug.

2.2.9. Swelling behaviour of nanoparticles

The swelling behaviour of nanoparticles in an alcoholic medium (ethanol) and in PBS (pH 7.4) with 0.5% sodium dodecyl sulfate (SDS) was studied. 20 mg of each type of nanoparticles was placed in 2 ml of ethanol and in 2 ml of PBS with 0.5% SDS for 24 h at a constant temperature (37 °C). The equillibrium swelling degree (W_∞) was obtained by weighing the swollen product after filtering the nanoparticles through a polyamide filter (0.2 μm, Sartorius, Goettingen, Germany) (Bernardo, Blanco, Olmo, & Teijón, 2002).

2.2.10. Estimation of drug content

In order to determine the loaded TMX in nanoparticles, two different methods were carried out. In the first one, the amount of TMX loaded into the nanoparticles was determined by calculating the difference between the initial concentration of TMX solution and the final concentration after the loading process. This amount was considered to be loaded in the nanoparticles. The second method consisted in a direct extraction of drug from TMX-loaded nanoparticles using methanol: 3 mg of TMX-loaded nanoparticles were suspended in 1 ml of methanol under stirring conditions during 5 h. After this time, the suspension was centrifuged (13,000 rpm, 5 min) and the supernatant was collected for the measurement. The samples obtained in both processes were analyzed by HPLC.

High performance liquid cromatography (HPLC) with fluorescence detector technique was required to determine the drug content (MacCallum, Cummings, Dixon, & Miller, 1996). The chromatographic separation was performed on a 25 cm × 4.6 mm RP-Spherisorb ODS2 C_{18} column (5 μm particle size, Waters). The mobile phase consisted of 1% aqueous dissolution of triethylamine and methanol 11/89 (v/v). A flow rate of 1 ml/min was established. The fluorescence detector was set at an excitation wavelength of 250 nm and an emission wavelength of 370 nm. A photoquemical reactor unit with a wavelength of 254 nm was placed between the detector and the column. Chromquest 4.2 software (Thermo) was used to process the obtained data. Standard solutions (10–2000 ng/ml) of TMX in methanol were used to obtain the calibration curve.

2.2.11. Thermogravimetric analysis (TGA)

TGA curves of drug-loaded and unloaded nanoparticles, as well as modified and unmodified materials, were obtained using a Mettler Toledo thermal analyzer (TGA-SDTA 851). The mass of the samples was 1.5 mg. The sample pan was placed onto the balance and the temperature was increased from 25 to 600 °C at a heating rate of 10 °C min^{-1} under nitrogen atmosphere (nitrogen flow rate of 60 cm^3 min^{-1}). The mass of the sample pan was continuously recorded as a function of temperature.

2.2.12. Drug release studies

For drug release studies from TMX-loaded nanoparticles, 5 mg of drug-loaded nanoparticles was added to 5 ml PBS with 0.5% SDS contained in a flask vial at a constant temperature (37 °C) and orbital shaking (100 rpm, Ecotron INFORS HT). TMX is relatively insoluble in the aqueous medium and SDS is an anionic surfactant used to make the release of the drug easier in phosphate buffer (Hu, Neoh, & Kang, 2006). At intervals, 50 μl samples were withdrawn from the solution in order to follow the change in drug concentration using HPLC. The removed volume from the vial was replaced with PBS with 0.5% SDS. Sink conditions were maintained during drug release experiments (Chawla & Amiji, 2002).

2.2.13. Mathematical modelling of release kinetics

In order to study the mechanism of drug release, the *in vitro* drug release data were fitted to various kinetic models: Higuchi, Korsemeyer–Peppas and partition phenomenon models were selected for the study (Blanco et al., 2008).

2.2.14. Statistical analysis

Statistical comparisons were performed with unpaired Student's *t*-test. A value of $p < 0.05$ was considered significant.

3. Results and discussion

3.1. Quantification of the thiol groups in the modified materials

The degree of modification was determined by measuring the amount of thiol groups of BSA and alginate using Ellmanïs reagent. The results showed an increase of sulfhydryl group content in both materials regarding unmodified materials. BSA has 17 intrachain disulfide bonds and 1 free sulfhydryl group. Hence, when the disulfide bonds are broken by a reduction process, modified BSA with more free sulfhydryl groups is supposed to be obtained (Kang, Kim, Shin, Woo, & Moon, 2003). BSA-SH displayed $3.1 \times 10^{-4} \pm 0.4 \times 10^{-4}$ mM of thiol groups per mg protein whereas unmodified BSA displayed $2.0 \times 10^{-5} \pm 0.6 \times 10^{-5}$ mM of thiol groups per mg protein (mean ± S.D.; $n = 7$). Thus, a BSA-SH with a concentration of thiol groups almost 15 times higher than the concentration of thiol groups of unmodified BSA was obtained.

Alginate exhibits a backbone of (1 → 4) linked β-D-mannuronic acid and α-L-guluronic acid residues of widely varying composition and sequence (Coviello, Matricardi, Marianecci, & Alhaique, 2007). Since the polymer displays carboxylic acid groups, the sulfhydryl compound L-cysteine can be easily covalently attached by the formation of amide bonds between the primary amino group of the amino acid and a carboxylic acid group of the polymer (Bernkop-Schnürch et al., 2001). ALG-CYS displayed $1.2 \times 10^{-3} \pm 0.2 \times 10^{-3}$ mM of thiol groups per mg polymer ($n = 7$). As unmodified alginate does not have sulfhydryl groups in its original structure, covalent attachment of L-cysteine was considered to have been a successful way to introducing thiol groups into the structure of alginic acid.

These thiolated polymers, or so-called thiomers, are polymers capable of forming disulfide bonds, the covalent bridging interaction most commonly encountered in biological systems, with different biological structures such as glycoproteins (Gum et al., 1992). Some studies showed these thiomers as a promising useful way for the noninvasive application of peptide drugs (Marschütz, Caliceti, & Bernkop-Schnürch, 2000).

3.2. Size and morphology of nanoparticles

Nanoparticles were obtained from BSA-SH and BSA-SH/ALG-CYS mixtures, but it was not possible to obtain them from ALG-CYS. FE-SEM micrographs of nanoparticles (Fig. 1) showed individual particles of very small size, most of them being nanometric. They showed cubic shape with certain spherical tendency, and their surface was smooth and without pores. Unlike polymeric nanoparticles such as poly-ε-caprolactone or poly(lactic-co-glycolic acid), polysaccharide-based nanoparticles are known to shrink and lose shape under electron bombardment during SEM analysis (Bilensoy et al., 2009). Thus, a less spherical shape in case of C-70-30 nanoparticles, whose composition included more proportion of ALG-CYS, could be attributed, at less in part, to this phenomenon (Fig. 1F).

Micrographs corresponding to optimization methods (Fig. 1C and D) showed individual particles with the same described features in both cases. Optimization of nanoparticle preparation process by desolvation has been used successfully in some studies (Langer et al., 2003; Weber et al., 2000). However, in this case results were considered more satisfactory by blocking with L-cysteine because more individual particles were found.

According to the obtained results, nanoparticles of Experiments 6, 7 and 8 (B-50-50, C-70-30 and BSA-SH, respectively; Table 1) were selected for the study of their average diameter and size distribution. All the obtained particles showed nanometric size. According to FE-SEM data, BSA-SH nanoparticles showed the smallest size (number-average diameter, $D_n = 96 \pm 52$ nm; polydispersity index, $U = 1.83$), followed by B-50-50 nanoparticles ($D_n = 186 \pm 73$ nm; $U = 1.53$). Finally, C-70-30 nanoparticles showed the largest size ($D_n = 306 \pm 74$ nm; $U = 1.19$). All the nanoparticle formulations were considered polydisperse, with a polydispersity index over 1.1 (Guerrero et al., 2008). Average diameters obtained with light-scattering (LS) technique confirmed this size characterization. BSA-SH, B-50-50 and C-70-30 nanoparticles showed an average diameter of 42, 189 and 388 nm, respectively. There were significant differences ($p < 0.05$) in the average diameter between all the nanoparticle formulations. Plots of size distributions, which were elaborated by measuring particles using micrograph enlargements and with LS technique, are represented in Fig. 2. Nanoparticles based on polysaccharides such as chitosan, and albumin nanoparticles, in a size range 150–300 nm, have shown good results as drug delivery systems in anticancer therapy (Bilensoy et al., 2009; Langer et al., 2003). Considering that the pore size of tumour microvessels varies from 100 to 1200 nm (Hobbs et al., 1998), the obtained size range of the nanoparticle formulations would allow the extravasation into tumour tissue.

3.3. Composition studies

The particle composition was studied evaluating the concentration of BSA-SH and ALG-CYS in the supernatant obtained after centrifugation in the synthesis process. Concentration of ALG-CYS in the supernatant was determined by a hydrolysis reaction of alginate and by measuring the absorbance of the obtained coloured products of this reaction at 277.6 nm. Hydrolysis conditions were extreme due to the high resistance of alginic acid to hydrolysis (Chandía, Matsuhiro, & Vásquez, 2001). Differences between standard curves of commercial alginate and ALG-CYS were not observed.

Concentration of BSA-SH in the supernatant was determined by a colorimetric reaction using Bradford's method. Differences between standard curves of commercial BSA and BSA-SH were not observed.

The absorbance of each sample was interpolated on the corresponding calibration curve, and the concentration of each polymer in the supernatant was obtained (Table 2). The percentage of each polymer incorporated into nanoparticles was calculated by the difference between the initial concentration in the synthesis process and the final concentration in the supernatant (Table 3). The BSA-SH/ALG-CYS ratio was calculated considering the concentration of each polymer incorporated into nanoparticles (Table 3).

A-50-50 and B-50-50 nanoparticles, which were only different in the weight of initial materials in the synthesis process, showed a similar value of BSA-SH/ALG-CYS ratio. It was concluded that modifications in amount of reactants in synthesis did not have influence on nanoparticle composition. Nanoparticles of C-70-30 synthesis, which were different in proportion of reactants in the synthesis process, showed a different value of BSA-SH/ALG-CYS ratio. It was concluded that modifications in proportion of reactants in synthesis were a determinant in nanoparticle composition.

3.4. FT-IR spectroscopy

Modified and unmodified materials, as well as BSA-SH/ALG-CYS nanoparticles, were analyzed by FT-IR spectroscopy, and their spectra were compared to observe possible differences due to chemical transformation (Fig. 3). Because signal from sulfhydryl groups and disulfide bonds is very weak (Socrates, 2004), and also due to the complex structure of the analyzed molecules, it was not possi-

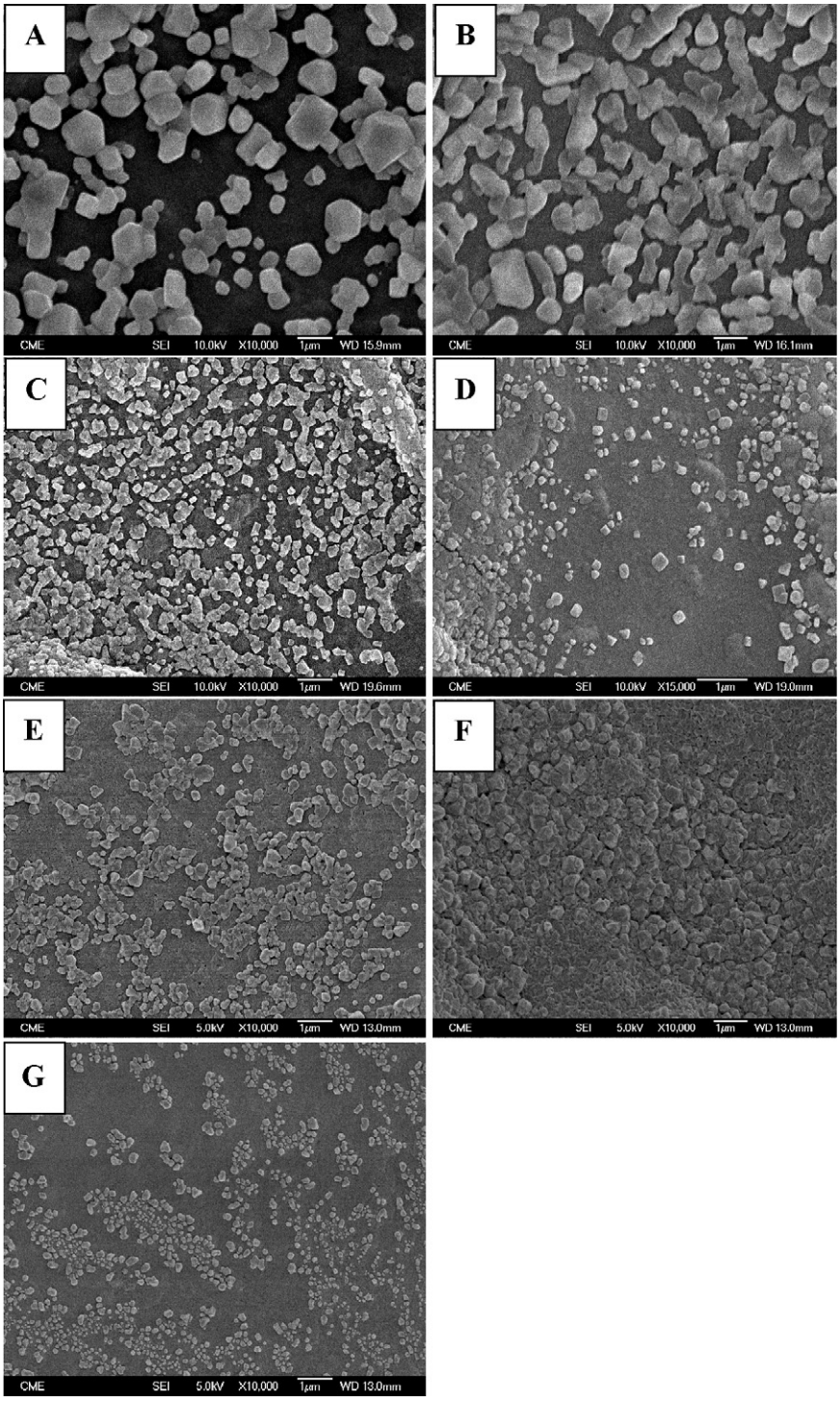

Fig. 1. FE-SEM micrographs of nanoparticles. Experiment 1; A-50-50 particles (A), Experiment 2; BSA-SH particles (B), Experiment 4; A-50-50 particles (C), Experiment 5; A-50-50 particles (D), Experiment 6; B-50-50 particles (E), Experiment 7; C-70-30 particles (F), Experiment 8; BSA-SH (G).

Table 2
Nanoparticle composition. Concentration and percentage of ALG-CYS and BSA-SH determined in the supernatant after the synthesis process. Percentage of each polymer incorporated into nanoparticles. BSA-SH/ALG-CYS ratio in nanoparticles.

Sample	ALG-CYS concentration in supernatant (mg/ml, %)	BSA-SH concentration in supernatant (mg/ml, %)	ALG-CYS incorporated into nanoparticles (%)	BSA-SH incorporated into nanoparticles (%)	BSA-SH/ALG-CYS ratio in nanoparticles
A 50-50; Experiment 1	2.891 ± 0.008[a] (57.8)	2.4 ± 0.4[a] (48.0)	42.2	52.0	1.23/1
B 50-50; Experiment 6	1.8 ± 0.3[a] (36.4)	1.3 ± 0.2[a] (26.8)	63.6	73.2	1.16/1
C 70-30; Experiment 7	3.38 ± 0.08[a] (48.3)	1.2 ± 0.2[a] (40.3)	51.7	59.7	0.49/1
BSA-SH; Experiment 8	–	0.68 ± 0.05[a] (6.8)	–	93.2	–

[a] Mean ± S.D. ($n = 3$).

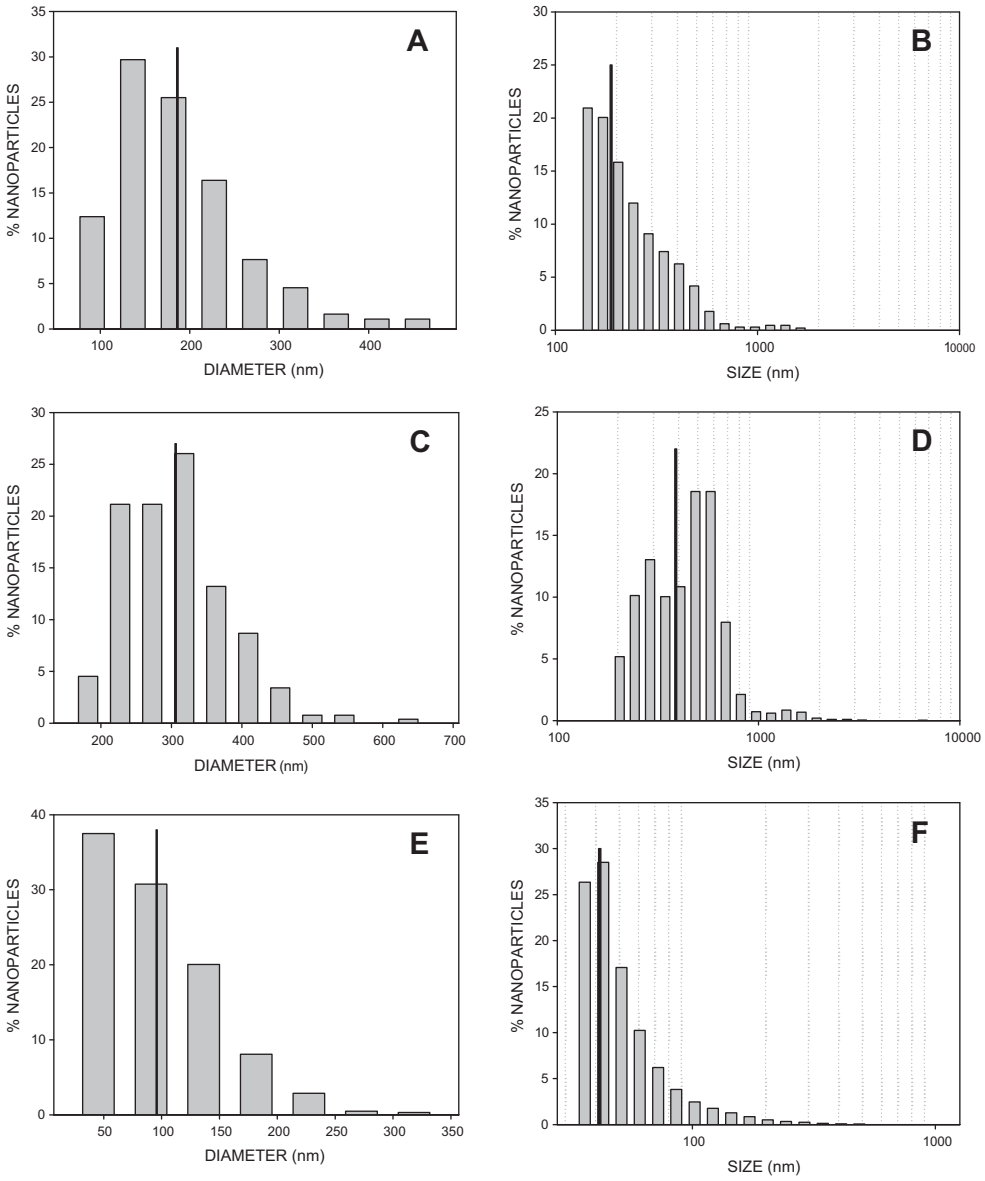

Fig. 2. Size distribution of nanoparticles of Experiment 6 (A and B), Experiment 7 (C and D) and Experiment 8 (E and F) by measuring particles using FE-SEM micrograph enlargements (A, C and E), and LS technique (B, D and E). Average diameter: solid line.

ble to identify the band of free sulfhydryl groups corresponding to chemical modifications in the materials. Instead of using this band, different bands were analyzed. Differences between spectra of both BSA were not observed because the only difference between them was the presence of more free sulfhydryl groups in BSA-SH (Fig. 3A). Amide I band (1700–1600 cm^{-1}) and amide II band (1550–1500 cm^{-1}), which are characteristic of peptide bonds (Maruyama et al., 2001), were identified in both spectra.

In the case of unmodified alginate and ALG-CYS, some differences between their spectra were found (Fig. 3B). The bands at 1617 and 1418 cm^{-1} in the IR spectrum of sodium alginate (unmodified alginate) were assigned to asymmetric and symmetric stretching peaks of carboxylate salt groups (Huang, Pal, & Moon, 1999). In the spectrum of ALG-CYS, bands at 1739, 1605, 1412 and 1248 cm^{-1} were observed due to the presence of –COOH groups, which are characteristic of alginic acid. Furthermore, two bands at 1687 and 1477 cm^{-1}, which were assigned to amide I band and amide III bands respectively, due to the presence of amide bonds formed with the introduction of molecules of L-cysteine in the original structure, were observed. The presence of different bands in the spectra of alginates allowed to confirm the chemical transformation of alginate.

Comparing BSA-SH/ALG-CYS nanoparticle spectrum with modified material spectra, it was observed that spectrum of nanoparticles was more similar to the BSA-SH spectrum, but with the presence of two bands at 1095 and 1032 cm^{-1}; these bands were assigned to the presence of ALG-CYS in the nanoparticle composition. Furthermore, the characteristic band of alginic acid at 1739 nm, which was present in ALG-CYS, disappears in the case of nanoparticle spectrum because the –COOH groups are in the salt form, and not in the acidic form as a consequence of the change of the pH in the synthesis process of nanoparticles. With this data, the presence of both modified materials in the structure of nanoparticles was confirmed.

3.5. Swelling behaviour of nanoparticles

The swelling behaviour of nanoparticles in an alcoholic medium (ethanol), and in PBS with SDS was studied. All the nanoparticle formulations showed a good swelling behaviour in both media. In

Table 3
Phenomenological data for the thermal descomposition of unmodified and modified materials (BSA, sodium alginate, BSA-SH and ALG-CYS), unloaded nanoparticles (A-50-50, B-50-50, C-70-30 and BSA-SH) and TMX-loaded nanoparticles (TMX B-50-50, TMX C-70-30 and TMX BSA-SH).

Sample	Mass loss (%) up to 600 °C	Peak temperature in DTG (°C)	Mass loss (%) in the step of thermal descomposition
BSA	83.5	306	40.3
BSA-SH	81.9	329	50.2
Sodium alginate	65.4	244	40.2
ALG-CYS	89.1	217	39.9
B-50-50 NP (Exp. 6)	100	235	30.8
		302	59.4
C-70-30 NP (Exp.7)	100	223.3	22.4
		301	50.3
BSA-SH NP (Exp.8)	100	302	47.5
TMX B-50-50 NP	100	240.8	21.5
		306	55
TMX C-70-30 NP	100	240.8	30.3
		304	55.8
TMX BSA-SH NP	86.5	314	47.3
TMX	100	258	68.9

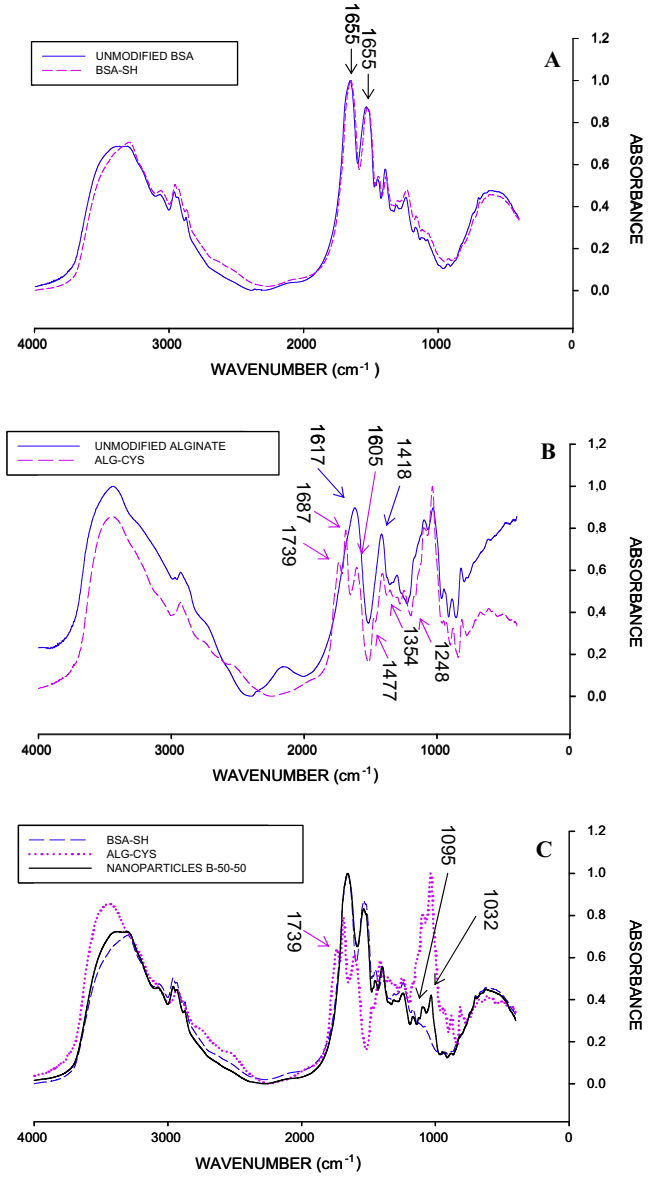

Fig. 3. FT-IR spectra of: BSA-SH and unmodified BSA (A), ALG-CYS and unmodified alginate (B), BSA-SH, ALG-CYS and B-50-50 nanoparticles (C).

PBS, W_∞ values of 93.8%, 93% and 95% were obtained for B-50-50, C-70-30 and BSA-SH nanoparticles, respectively. In ethanol, W_∞ values of 88.2%, 88.7% and 80.4% were obtained for B-50-50, C-70-30 and BSA-SH systems, respectively. Hence, BSA-SH nanoparticles were more swollen in PBS than in ethanol, in contrast with B-50-50 and C-70-30 nanoparticles which were more swollen in ethanol than in PBS. These results suggest that the presence of ALG-CYS in the nanoparticle composition makes nanoparticle swelling in an alcoholic medium easier than in PBS.

3.6. Estimation of drug content

Two different methods were carried out to determine the drug content. One of them considered the difference between the initial concentration of TMX solution and the final concentration after the loading process of the drug. The other one consisted in the quantification of a direct extraction of TMX from drug-loaded nanoparticles with methanol. The obtained drug content detected with each method is shown in Table 4. According to the data obtained with both methods, TMX B-50-50 and TMX C-70-30 nanoparticles included more drug than TMX BSA-SH nanoparticles. Thus, the difference in the composition of nanoparticles was an important factor in the drug-loading process. As described previously, swelling behaviour of nanoparticle formulations was related to the nanoparticle composition. Nanoparticles with ALG-CYS in their composition could include more drug than BSA-SH nanoparticles because of their higher swelling in an alcoholic medium. The amount of loaded TMX seems to be different depending on the method (Table 4). Considering the results, direct extraction of drug from nanoparticles with methanol allowed only part of the TMX to be included in the particles. TMX is a very hydrophobic drug and it has strong interactions with the hydrophobic regions of the albumin and other plasma proteins (>95%) (Morello, Wurz, & DeGregorio, 2003). As a consequence of these interactions, methanol could only extract the superficial tamoxifen of nanoparticles whose interactions with albumin were weaker. Furthermore, as a consequence of the swelling degree and composition of each nanoparticle formulation, the amount of tamoxifen extracted with methanol in case of TMX C-70-30 and TMX B-50-50 nanoparticles was similar and higher than that in the case of TMX BSA-SH nanoparticles.

3.7. Thermogravimetric study

The thermal stability of modified materials, drug-loaded and unloaded nanoparticles was studied. The TGA first derivative of the materials is plotted in Fig. 4, and the parameters derived from them are collected in Table 3. Differences between the thermal behaviour of modified and unmodified materials were observed. Modified albumin and alginate-cysteine degraded in a one-step process at a maximum temperature of 329 and 217 °C, respectively, which are different from the degradation temperatures of unmodified materials (Fig. 4A, B and Table 3). There were differences in the percentage of total mass loss between modified and unmodified polymers (Table 3). These differences in thermal behaviour of modified and unmodified materials again confirmed the chemical modification. BSA-SH (Experiment 8) nanoparticles degraded in a one-step process at a maximum temperature of 302 °C (Fig. 4C and Table 3) in contrast with B-50-50 and C-70-30, which degraded in two different steps (Fig. 4C and Table 3). The first degradation step of B-50-50 and C-70-30 nanoparticles occurred at 235 and 223.3 °C, respectively, being these temperatures very similar to the degradation temperature of ALG-CYS (Table 3). The second degradation step occurred at 302 and 301 °C, respectively, being these temperatures close to the degradation temperature of BSA-SH. The two-step degradation process of the nanoparti-

Table 4
Estimation of tamoxifen content in nanoparticles.

Sample	Drug content in nanoparticles		
	By difference of concentration in drug-solution after loading process (μg TMX/mg NP)	By TMX extraction with methanol (μg TMX/mg NP)	Percentage of TMX extracted with methanol (%)
TMX B-50-50	$3.9 \pm 0.5^{a,b,*}$	$2.1 \pm 0.5^{a,c,*}$	53.8
TMX C-70-30	$4.3 \pm 0.2^{d,e,*}$	$1.9 \pm 0.3^{d,f,*}$	44.2
TMX BSA-SH	$2.1 \pm 0.5^{b,e,g,*}$	$0.7 \pm 0.08^{c,f,g,*}$	33.3

Data marked with the same letter showed significant differences between them.
* Mean ± S.D. ($n = 3$).

cles composed by ALG-CYS and BSA-SH confirmed the presence of both materials in these nanoparticles, in contrast with BSA-SH nanoparticles which showed a similar behaviour to BSA-SH. The thermal behaviour of TMX-loaded nanoparticles was very similar to the unloaded nanoparticles (Fig. 4D and Table 5), allowing it to conclude that the presence of TMX in the drug-loaded nanoparticles did not cause significant modifications in the stability of particles.

3.8. Drug release studies

The release of TMX from drug-loaded nanoparticles is shown in Fig. 5. The maximum drug release from TMX-B-50-50 was 1.3 ± 0.1 μg TMX per mg nanoparticle at 7 h (Fig. 5A); from TMX C-70-30 it was 2.64 ± 0.06 μg TMX per mg nanoparticle at 26.5 h (Fig. 5B); and from TMX BSA-SH, 0.50 ± 0.01 μg TMX per mg nanoparticle at 75 h (Fig. 5C).

Three stages in drug release were established and the release rate in each stage was determined (Table 5). The drug release occurred in a short first stage which was the fastest one, followed by a second stage which was slower and longer than the first one. From this, a very slow release rate was observed in all cases. Comparing the release rate in the first stage of each nanoparticle formulation, TMX release was faster from TMX C-70-30 and TMX B-50-50, and slower from TMX BSA-SH (Table 5). The release rate in the second stage became much slower in all cases. Different studies in which TMX was incorporated into nanoparticles based on synthetic polymers, such as poly(ε-caprolactone) or poly(ethylene-glycol)-modified cyanoacrilate, showed a fast release of the drug in the first hours, and the total release of the drug within a 24-h time interval. The burst release of hydrophobic drugs, like TMX, was attributed to the predominant surface presence of the drug in the nanoparticle formulation (Chawla & Amiji, 2002). In BSA-SH/ALG-CYS and BSA-SH nanoparticles, this fast release of TMX could be

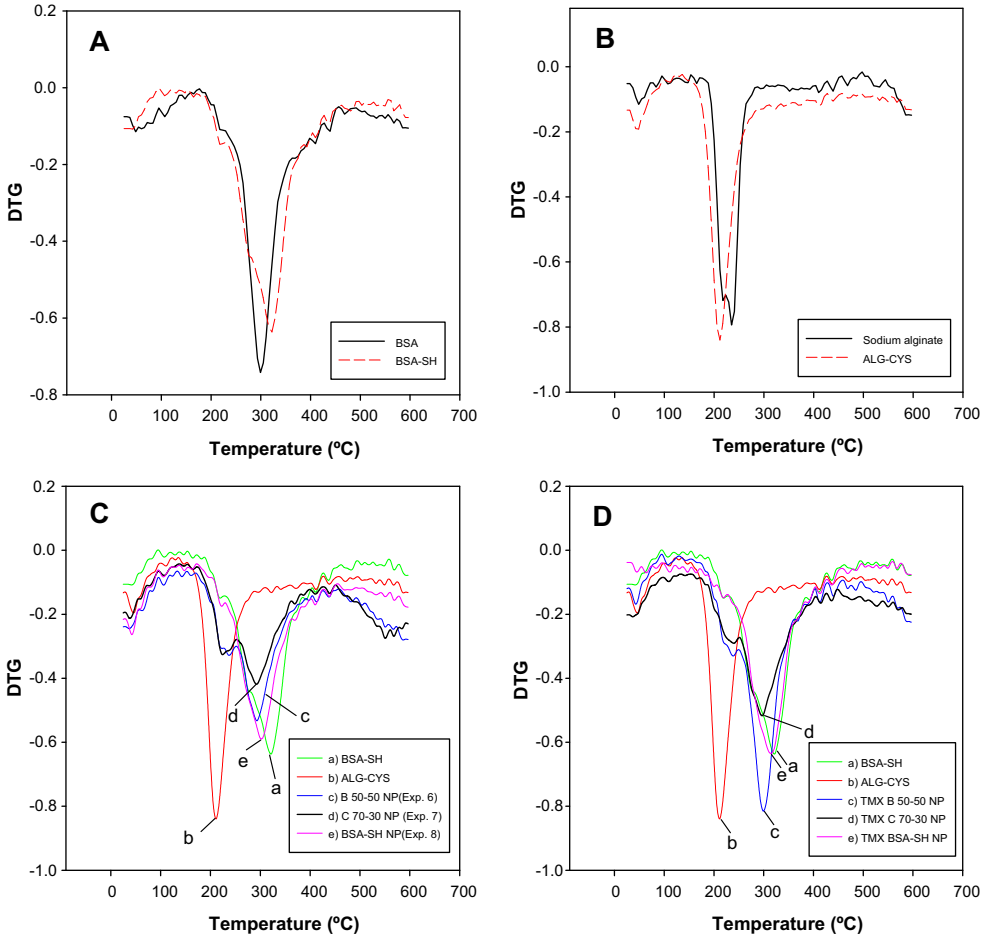

Fig. 4. TGA first derivative curves of modified and unmodified BSA (A), modified and unmodified alginate (B), unloaded nanoparticles and modified materials (C) and tamoxifen-loaded nanoparticles and modified materials (D).

Table 5
Release rates of tamoxifen from nanoparticle formulations.

Sample	First stage		Second stage	
	K (μg TMX/mg NP/h)	Time (min)	*K* (μg TMX/mg NP/h)[a]	Time (h)
TMX B-50-50	2.90 (0.890)	0–10	0.31 (0.948)	0.5–2
TMX C-70-30	2.72 (0.983)	0–30	0.22 (0.916)	1–4
TMX BSA-SH	0.15 (0.999)	0–30	0.027 (0.972)	1–8

[a] Value in parenthesis is r^2.

observed in the first stage. Hence, it was concluded that superficial TMX, whose interactions with the nanoparticles were weaker, was released in the first stage. Thus, nanoparticles with ALG-CYS in their composition showed a faster first stage than BSA-SH nanoparticles. In the second stage, TMX strongly retained by the nanoparticles was released. Thus, the release rate became much slower in second stage. From this, the release rate in all the cases became much slower. In contrast with the mentioned studies, in any case the total release of the loaded drug was achieved. It was concluded that interactions between TMX and albumin were the main regulator factor in the release of the drug and, because these interactions were very strong, total release of the drug was not achieved. This partial release of TMX could be an advantage if these drug-loaded nanoparticles were intravenously administered, since they could be uptake by cells with a significant amount of antitumoural drug.

3.9. Mathematical modelling of release kinetics

The mechanism of drug release through the mathematical modelling of dissolution data for the drug delivery systems was evaluated. The regression parameters (release kinetic constants and regression coefficients) obtained after fitting the kinetic models to the *in vitro* drug release data are given in Table 6. Modelling analysis was carried out by fitting the data until the time when a minimum 73%, 81% and 97% of drug was released from TMX BSA-SH, TMX C-70-70 and TMX B-50-50 nanoparticles, respectively. According to the obtained results, formulations were observed to yield statistically valid correlations with various models (Table 6).

The drug release studies of the three nanoparticle formulation were in accordance with the square root of time, since all formulations showed good correlation with the Higuchi model.

According to the Korsemeyer–Peppas model, in cases of pure Fickian release the exponent *n* has the limiting values of 0.5, 0.45 and 0.43 for release from slabs, cylinders and spheres, respectively. For drug release from spherical polymer particles of a wide size distribution, the value of the exponent *n* for Fickian diffusion depends on the width of the distribution (Ritger & Peppas, 1987), and *n* values lower than 0.43 can be obtained. The obtained values of the diffusional exponent *n* for TMX B-50-50 and TMX BSA-SH nanoparticles were lower than 0.43, probably because of the wide size

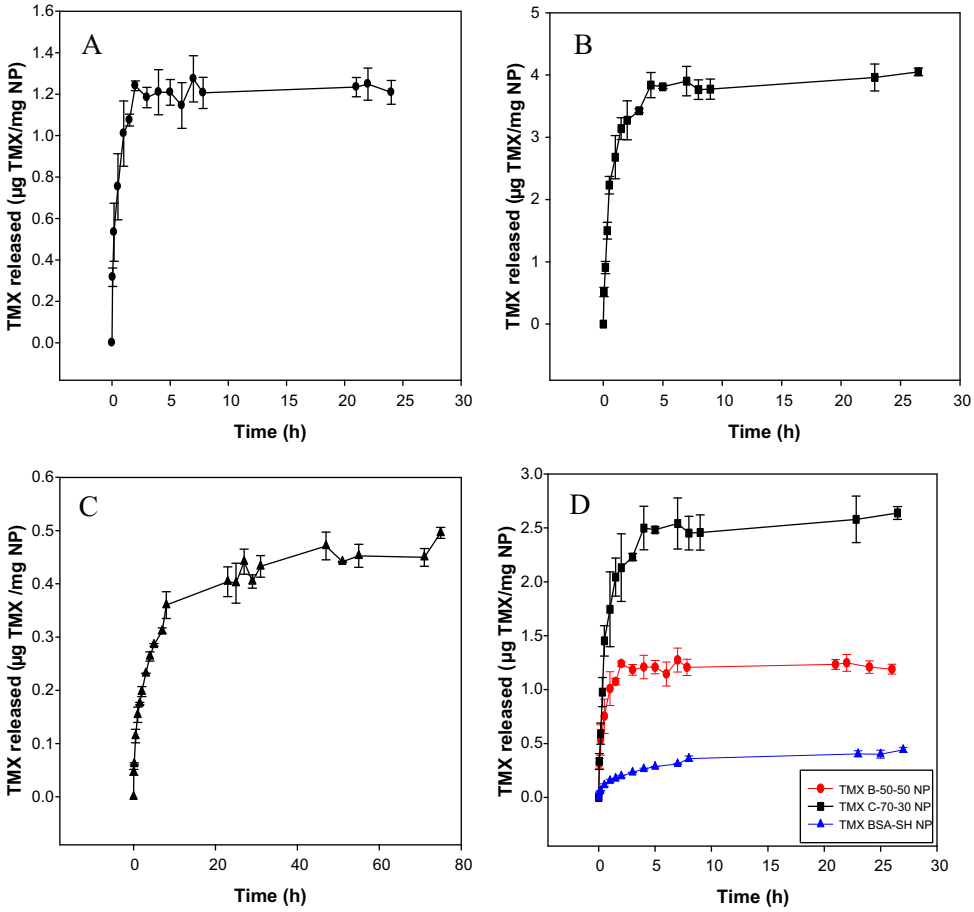

Fig. 5. Cumulative amount of TMX released from drug-loaded TMX B-50-50 (A), TMX C-70-30 (B) and TMX BSA-SH (C) nanoparticles. Comparison of the three release curves during the first 24 h (D).

Table 6
Statistical parameters of various formulations obtained after fitting the drug release data to the release kinetic models. Model fitting was reattempted until a minimum of 73%, 81% and 97% of drug release from TMX BSA-SH, TMX C-70-70 and TMX B-50-50 nanoparticles, respectively.

Formulation	Higuchi K ($h^{-1/2}$)[a]	Korsemeyer–Peppas n[a]	Partition phenomenon (first order) k_R (h^{-1})[a]	Partition phenomenon (second order) k_R (h^{-1})[a]	M_t/M_∞ versus t^n; $n = 0.5$ K ($h^{-1/2}$)[a]
TMX B-50-50	0.834 (0.973)	0.36 (0.995)	0.506 (0.938)	2.674 (0.938)	0.654 (0.973)
TMX C-70-30	1,613 (0.970)	0.53 (0.972)	3.154 (0.898)	3.15 (0.898)	0.485 (0.932)
TMX BSA-SH	0.119 (0.989)	0.412 (0.993)	0.035 (0.982)	0.128 (0.990)	0.241 (0.989)

[a] Value in parenthesis is r^2.

distribution. In case of TMX C-70-30, the obtained value of n is closer to 0.5 than 0.43. This could be explained because C-70-30 nanoparticle shape was less spherical and had more slab form (see Fig. 1F).

As all the formulations showed good correlation for the Higuchi and Korsemeyer–Peppas models, an approximation of this last model was made in order to confirm the Fickian diffusion component in the release of the drug (Chung, Lin, Liu, Tyan, & Yang, 2009). Korsemeyer–Peppas model was applied considering in all cases the presence of Fickian diffusion (M_t/M_∞ versus t^n; $n = 0.5$). The results are shown in Table 6, showing in all cases good correlation for the approximation. According to the results of the application of Higuchi, Korsemeyer–Peppas model and the approximation to a Fickian release of Korsemeyer–Peppas model, it was declared a Fickian release behaviour for all the formulations.

In accordance with the mathematical model proposed by Reis, Guilherme, Rubira, and Muniz (2007), the loading of solutes onto and their release from hydrogel-based devices can be better understood when they are treated as a partition phenomenon. Two possibilities were considered: one is that solute release follows reversible first-order kinetics, and the second option is that solute release follows reversible second-order kinetics (Blanco et al., 2008). According to the high swelling degree of all the formulations in PBS with 0.5% SDS, this model was applied in order to confirm a hydrogel behaviour of nanoparticles. After fitting this mathematical model, it was concluded the presence of a partition phenomenon in TMX BSA-SH and TMX B-50-50, where the albumin had a higher presence in composition of nanoparticles and whose swelling degrees in PBS with 0.5% SDS were higher.

4. Conclusion

Disulfide bond reduced albumin BSA and ALG-CYS were successfully obtained. Nanoparticles based on BSA-SH and BSA-SH/ALG-CYS mixtures have been prepared and characterized. Individual particles with certain spherical tendency and small size (<300 nm) were obtained in all cases. Modifications in proportion of reactants in the synthesis process were determinant in nanoparticle composition. FT-IR and TGA studies confirmed the composition and stability of nanoparticles, as well as the chemical modification and stability of modified materials. The presence of ALG-CYS in the nanoparticle composition conditioned the swelling behaviour of nanoparticles. TMX was successfully incorporated into nanoparticles, and nanoparticle composition conditioned the drug content in nanoparticles (2–4 μg/mg), as well as the amount and the rate of drug released. Interactions between the drug and nanoparticle structure conditioned the release of TMX. Total release of the drug was not achieved in any case; only the 23–61% of the drug was released. After fitting several mathematical models, a Fickian release behaviour for all the formulations was declared. According to the obtained results, these nanoparticle formulations are potential candidates as drug delivery systems for antitumour drug administration.

Acknowledgements

The financial support of the Ministerio de Ciencia e Innovación of Spain (PS09/01513), of the Fundación Mutua Madrileña and the FPI grant from UCM to A. Martínez are gratefully acknowledged.

References

Ameller, T., Legrand, P., Marsaud, V., & Renoir, J. M. (2004). Drug delivery systems for oestrogenic hormones and antagonists: The need for selective targeting in estradiol-dependent cancers. *The Journal of Steroid Biochemistry and Molecular Biology*, *92*(1–2), 1–18.

Bernardo, M. V., Blanco, M. D., Olmo, R., & Teijón, J. M. (2002). Delivery of bupivacaine included in poly(acrylamide-co-monomethyl itaconate) hydrogels as a function of the pH swelling medium. *Journal of Applied Polymer Science*, *86*, 327–334.

Bernkop-Schnürch, A., Kast, C. E., & Richter, M. F. (2001). Improvement in the mucoadhesive properties of alginate by the covalent attachment of cysteine. *Journal of Controlled Release*, *71*(3), 277–285.

Bilensoy, E., Sarisozen, C., Esendagli, G., Dogan, A. L., Aktas, Y., Sen, M., et al. (2009). Intravesical cationic nanoparticles of chitosan and polycaprolactone for the delivery of Mitomycin C to bladder tumors. *International Journal of Pharmaceutics*, *371*(1–2), 170–176.

Blanco, M. D., Guerrero, S., Teijón, C., Olmo, R., Pastrana, L., Katime, I., et al. (2008). Preparation and characterization of nanoparticulate poly(N-isopropylacrylamide) Hydrogel for the controlled release of anti-tumour drugs. *Polymer International*, *57*, 1215–1225 (Erratum: Polymer International, 2009, 58, 116).

Bradford, M. M. (1976). A rapid and sensitive method for the quantitation of microgram quantities of protein utilizing the principle of protein-dye binding. *Analytical Biochemistry*, *72*, 248–254.

Brigger, I., Dubernet, C., & Couvreur, P. (2002). Nanoparticles in cancer therapy and diagnosis. *Advanced Drug Delivery Reviews*, *54*(5), 631–651.

Chandía, N. P., Matsuhiro, B., & Vásquez, A. E. (2001). Alginic acids in *Lessonia trabeculata*: characterization by formic acid hydrolysis and FT-IR spectroscopy. *Carbohydrate Polymers*, *46*, 81–87.

Chawla, J. S., & Amiji, M. M. (2002). Biodegradable poly(ε-caprolactone) nanoparticles for tumor-targeted delivery of tamoxifen. *International Journal Pharmaceutics*, *249*(1–2), 127–138.

Chung, T. W., Lin, S. Y., Liu, D. Z., Tyan, Y. C., & Yang, J. S. (2009). Sustained release of 5-FU from Poloxamer gels interpenetrated by crosslinking chitosan network. *International Journal of Pharmaceutics*, *382*(1–2), 39–44.

Coviello, T., Matricardi, P., Marianecci, C., & Alhaique, F. (2007). Polysaccharide hydrogels for modified release formulations. *Journal of Controlled Release*, *119*(1), 5–24.

Ellman, G. L. (1959). Tissue sulfhydryl groups. *Archives of Biochemistry and Biophysics*, *82*(1), 70–77.

Guerrero, S., Muñiz, E., Teijon, C., Olmo, R., Teijon, J. M., & Blanco, M. D. (2008). Ketotifen-loaded microspheres prepared by spray-drying poly(D,L-lactide) and poly(D,L-lactide-co-glycolide) polymers: characterization and in vivo evaluation. *Journal of Pharmaceutical Sciences*, *97*(8), 3153–3169.

Gum, J. R., Jr., Hicks, J. W., Toribara, N. W., Rothe, E. M., Lagace, R. E., & Kim, Y. S. (1992). The human MUC2 intestinal mucin has cysteine-rich subdomains located both upstream and downstream of its central repetitive region. *The Journal of Biological Chemistry*, *267*(30), 21375–21383.

Hobbs, S. K., Monsky, W. L., Yuan, F., Roberts, W. G., Griffith, L., Torchilin, V. P., et al. (1998). Regulation of transport pathways in tumor vessels: role of tumor type and microenvironment. *Proceedings of the National Academy of Sciences of the United States of America*, *95*(8), 4607–4612.

Hu, F. X., Neoh, K. G., & Kang, E. T. (2006). Synthesis and in vitro anti-cancer evaluation of tamoxifen-loaded magnetite/PLLA composite nanoparticles. *Biomaterials*, *27*(33), 5725–5733.

Huang, R. Y. M., Pal, R., & Moon, G. Y. (1999). Characteristics of sodium alginate membranes for the pervaporation dehydration of ethanol–water and isopropanol–water mixtures. *Journal of Membranes Science*, *160*, 101–113.

Kang, Y. N., Kim, H., Shin, W. S., Woo, G., & Moon, T. W. (2003). Effect of disulfide bond reduction on bovine serum albumin-stabilized emulsion gel formed by microbial transglutaminase. *Journal of Food Science*, *68*(7), 2215–2220.

Karmali, P. P., Kotamraju, V. R., Kastantin, M., Black, M., Missirlis, D., Tirrell, M., et al. (2009). Targeting of albumin-embedded paclitaxel nanoparticles to tumors. *Nanomedicine*, *5*(1), 73–82.

Kratz, F. (2008). Albumin as a drug carrier: design of prodrugs, drug conjugates and nanoparticles. *Journal of Controlled Release*, *132*(3), 171–183.

Langer, K., Balthasar, S., Vogel, V., Dinauer, N., von Briesen, H., & Schubert, D. (2003). Optimization of the preparation process for human serum albumin (HSA) nanoparticles. *International Journal of Pharmaceutics*, *257*(1–2), 169–180.

MacCallum, J., Cummings, J., Dixon, J. M., & Miller, W. R. (1996). Solid-phase extraction and high-performance liquid chromatographic determination of tamoxifen and its major metabolites in plasma. *Journal of Chromatography B: Biomedical Application*, *678*(2), 317–323.

Marschütz, M. K., & Bernkop-Schnürch, A. (2002). Thiolated polymers: self-crosslinking properties of thiolated 450 kDa poly(acrylic acid) and their influence on mucoadhesion. *European Journal of Pharmaceutical Sciences*, *15*(4), 387–394.

Marschütz, M. K., Caliceti, P., & Bernkop-Schnürch, A. (2000). Design and in vivo evaluation of an oral delivery system for insulin. *Pharmaceutical Research*, *17*(12), 1468–1474.

Maruyama, T., Katoh, S., Nakajima, M., Nabetani, H., Abbott, T. P., Shono, A., et al. (2001). FTIR analysis of BSA fouled on ultrafiltration and microfiltration membranes. *Journal of Membrane Science*, *192*, 201–207.

Moghimi, S. M., Hunter, A. C., & Murray, J. C. (2005). Nanomedicine: current status and future prospects. *FASEB Journal*, *19*(3), 311–330.

Morello, K. C., Wurz, G. T., & DeGregorio, M. W. (2003). Pharmacokinetics of selective estrogen receptor modulators. *Clinical Pharmacokinetics*, *42*(4), 361–372.

Reis, A. V., Guilherme, M. R., Rubira, A. F., & Muniz, E. C. (2007). Mathematical model for the prediction of the overall profile of in vitro solute release from polymer networks. *Journal of Colloid and Interface Science*, *310*(1), 128–135.

Ritger, P. L., & Peppas, N. A. (1987). A simple equation for description of solute release. I: Fickian and non-Fickian release from non-swellable devices in the form of slabs, spheres, cylinders or discs. *Journal of Controlled Release*, *5*, 23–36.

Socrates, G. (2004). *Infrared and Raman characteristic group frequences: tables and charts* (3th ed.). John Wiley & Sons Ltd., p. 16.

Weber, C., Coester, C., Kreuter, J., & Langer, K. (2000). Desolvation process and surface characterisation of protein nanoparticles. *International Journal of Pharmaceutics*, *194*(1), 91–102.

Yoshioka, T., Ikoma, T., Monkawa, A., Yunoki, S., Abe, T., Sakane, M., et al. (2007). Preparation of hydroxyapatite-alginate gels as a carrier for controlled release of paclitaxel. *Key Engineering Materials*, *330–332*, 1053–1056.